Evidence of coupling between phonons and charge-density waves in $ErTe_3$

N. Lazarević and Z. V. Popović
Center for Solid State Physics and New Materials, Institute of Physics, University of Belgrade, Pregrevica 118, 11080 Belgrade, Serbia

Rongwei Hu* and C. Petrovic
Condensed Matter Physics and Materials Science Department, Brookhaven National Laboratory, Upton, New York 11973-5000, USA
(Received 24 September 2010; revised manuscript received 2 November 2010; published 24 January 2011)

The vibrational properties of $ErTe_3$ were investigated using Raman spectroscopy and were analyzed on the basis of peculiarities of the RTe_3 crystal structure. Four Raman active modes for the undistorted structure, predicted by factor-group analysis, are experimentally observed and assigned according to diperiodic symmetry of the $ErTe_3$ layer. By analyzing temperature dependence of the Raman mode energy and intensity, we have provided clear evidence that all Raman modes, active in the normal phase, are coupled to the charge-density waves. In addition, new modes have been observed in the distorted state.

DOI: 10.1103/PhysRevB.83.024302 PACS number(s): 78.30.−j, 71.45.Lr, 63.20.K−

I. INTRODUCTION

Low-dimensional systems with highly anisotropic electronic structure often exhibit electronic instabilities that can lead to superconductivity or charge-density waves (CDW). CDW can be created through a Fermi surface (FS) nesting effect. If the FS can be nested with one q vector of a particular phonon mode, the ground-state energy can be reduced by electron-phonon coupling, resulting in gaps opening at the FS and the creation of a new ground state with broken symmetry. FS for an ideal one-dimensional system consists of two points, so it exhibits perfect nesting at $q = 2k_f$. In real systems, good nesting is reduced only to some parts of the FS. In these cases, the CDW gap is expected to open only on the best nested FS parts, and the system can remain metallic in its new ground state.

In recent years, the high-temperature CDW family of rare-earth tritellurides (RTe_3) have attracted much attention.[1] A wide range of tunable parameters in the RTe_3 offers unique opportunity for the study of the CDW formation.[2–7] For the layered quasi-2-D material with tetragonal symmetry, the CDW ground state can either be bidirectional (checkerboards) or unidirectional (stripes) with a reduced symmetry.[8] The high-resolution X-ray diffraction,[5–7] angle-resolved photoemission spectroscopy[9,10] and femtosecond pump-probe spectroscopy[11] showed that lighter rare-earth tritellurides (i.e., R = La − Tb) host unidirectional incommensurate CDW well above room temperature. For the heavy rare-earth tritellurides (i.e., R = Dy − Tm), transition temperature T_{CDW_1} ($T_{CDW_1} = 265$ K for $ErTe_3$) resides below room temperature, with another transition to a bidirectional CDW state at T_{CDW_2} ($T_{CDW_2} = 158$ K for $ErTe_3$).[7,12]

The Raman scattering measurements of RTe_3 were analyzed, to the best of our knowledge, only in Refs. 13 and 14. Lavagnini *et al.*[13] reported the Raman scattering spectra of RTe_3 (R = La, Ce, Pr, Nd, Sm, Gd, Dy) at ambient pressure and high-pressure Raman spectra of $LaTe_3$ and $CeTe_3$. In the case of the room-temperature Raman spectra of $LaTe_3$, they observed five modes at about 72, 88, 98, 109, and 136 cm^{-1} and labeled them as P1–P5. Polarization-dependent measurements showed that the P4 peak at about 109 cm^{-1} has 90° intensity change periodicity. They concluded that this mode cannot be assigned within the undistorted structure and consequently assigned it as the B_1 symmetry mode of the distorted structure.[13] In Ref. 14, amplitudon modes are observed and analyzed for $DyTe_3$ and $LaTe_3$.

In this article, we have measured Raman scattering spectra of $ErTe_3$ in normal and in CDW states. Our polarization-dependent Raman scattering measurements above T_{CDW_1} showed that the P_4 mode,[13] at about 120 cm^{-1}, persists in the normal state of $ErTe_3$. Appearance of this mode in the normal state and its B_{1g}symmetry lead us to a conclusion that the orthorhombic symmetry of the crystal does not play a dominant role in the phonon properties of RTe_3. We have found that factor group analysis of the layer symmetry predicts $3A_{1g} + B_{1g}$modes to be observed in Raman scattering experiments from the (010) plane of $ErTe_3$, in complete agreement with experimental findings. Temperature dependance of Raman mode energies and intensities have shown strong coupling of phonons with the CDW gaps.

II. EXPERIMENT

Single crystals of $ErTe_3$ were grown using the flux method.[15] The Raman scattering measurements were performed using a Jobin Yvon T64000 Raman system in micro-Raman configuration. The 514.5-nm line of an Ar^+/Kr^+ mixed gas laser was used as an excitation source. All Raman scattering measurements presented in this work were performed from the (010) plane of $ErTe_3$ single crystals. Low-temperature measurements were performed using a KONTI CryoVac continuous Helium flow cryostat with a 0.5-mm-thick window. Focusing of the laser beam was realized with a long-distance microscope objective (magnification 50×). We have found that laser power level of 0.01 mW on the sample is sufficient to obtain a Raman signal and, except for the signal-to-noise ratio, no changes of the spectra were observed as a consequence of laser heating by further lowering the laser power. The corresponding excitation power density was less then 0.05 kW/cm^2.

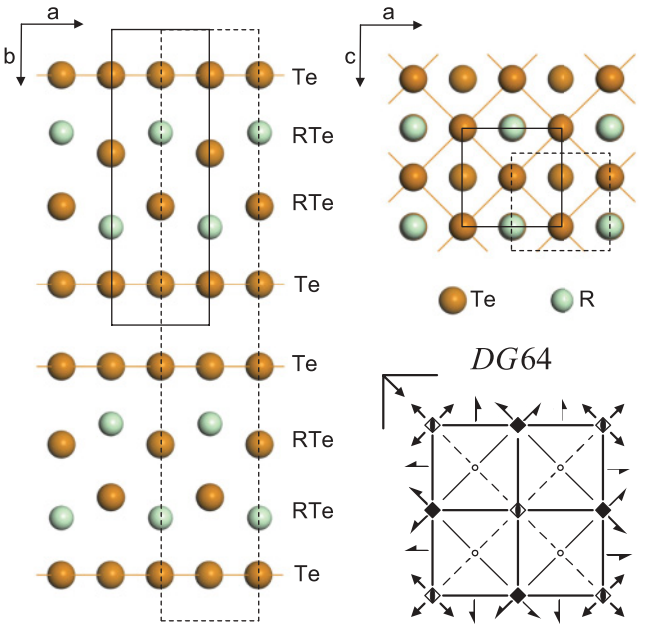

FIG. 1. (Color online) Schematic of RTe_3 crystal structure. Dashed lines represent the unit cell of RTe_3 crystal structure. The unit cell of the single RTe_3 layer is represented with solid lines. (bottom right) The diagram represents symmetry operations of the DG 64 diperiodic symmetry group.[17]

III. RESULTS AND DISCUSSION

$ErTe_3$ crystallizes in the $Cmcm$ (D_{2h}^{17}) space group orthorhombic structure with unit cell parameters $a = 4.31$ Å, $b = 24.45$ Å, $c = 4.31$ Å, and $Z = 4$.[16] All ions are in the c Wyckoff position (C_{2v} site symmetry).[16] The unit cell of the $ErTe_3$ crystal structure (Fig. 1) is built up of corrugated double layers of ErTe sandwiched by planar square nets of Te making $ErTe_3$ slabs stacked along the b axis. These slabs are mutually connected only by van der Waals forces.[4]

Factor group analysis (FGA) for the crystal symmetry gives the normal-mode distribution, $\Gamma = 4A_g + 4B_{1g} + 4B_{3g} + B_{1u} + B_{2u} + B_{3u}$. Based on the corresponding Raman tensors and the selection rules (see Fig. 2), we found that only A_g symmetry modes can be observed for our experimental configuration, in which both incident and scattered light are polarized parallel to the (ac) crystal plane.

Figure 3(a) shows room-temperature Raman scattering spectra of $ErTe_3$ (normal state) measured in parallel polarization for different orientations of the sample. By changing an angle between incident light polarization and the crystal axes (by rotating the sample), one can find the position at which the Raman mode at about 120 cm^{-1} disappears. The disappearance of this mode is shown to be periodical, with a period of 90° [see inset in Fig. 3(a)]. The same type of behavior was observed for the P_4 mode in Ref. 13 for $LaTe_3$ in the CDW state. Since periodicity of the A_g mode intensity change for the orthorhombic symmetry is 180°, the P_4 mode cannot be assigned within the orthorhombic crystal symmetry. Because the crystal structure of RTe_3 consists of two RTe_3 layers mutually connected by weak van der Waals forces, it is natural to expect that layer symmetry dominates in vibration properties of RTe_3.

Layered crystals can be properly treated as molecular crystals in which the molecular unit is a sheet extended infinitely in two dimensions.[18] Considering the vibrational properties of the individual layers, we break the periodicity in the direction perpendicular to the layer. Thus, for considering symmetry-related properties of the layer, we have to use the diperiodic groups in three dimensions.[17]

The structure of the $ErTe_3$ slab is shown in Fig. 1. The diperiodic symmetry group that fully describes symmetry of the $ErTe_3$ layer is DG 64, with two formula units ($Z = 2$) per unit cell. Two R and two Te atoms are in c (C_{4v} site symmetry), and four Te atoms are in f (C_{2v} site symmetry) Wyckoff positions. FGA for the $ErTe_3$ slab gives $\Gamma = 3A_{1g} + B_{1g} + 3A_{2u} + B_{2u} + 4E_g + 4E_u$. There are four

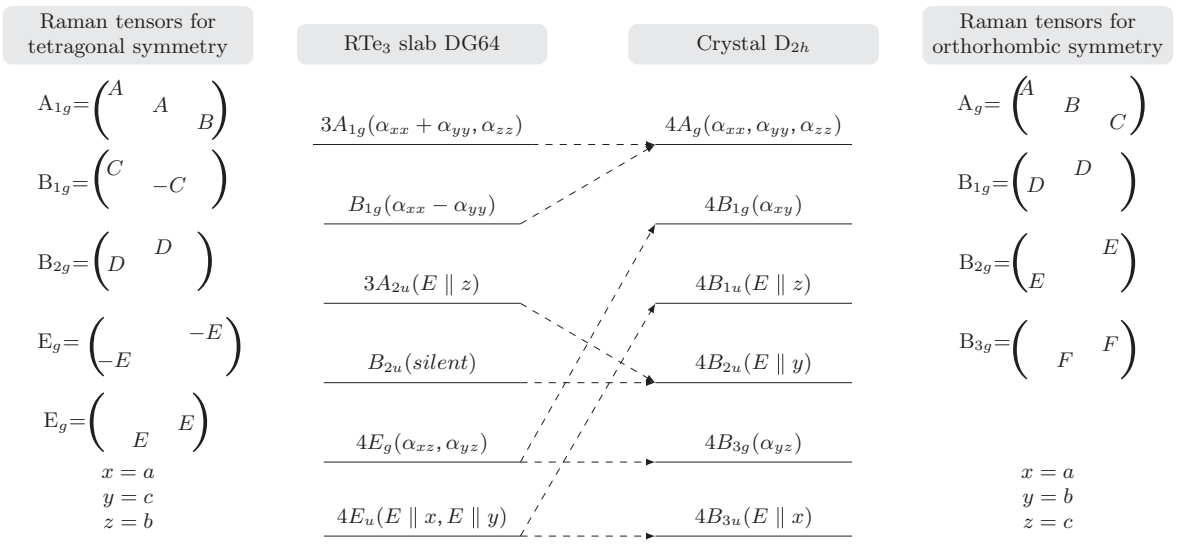

FIG. 2. Raman tensors and compatibility relations for the layer and the crystal symmetry of the RTe_3.

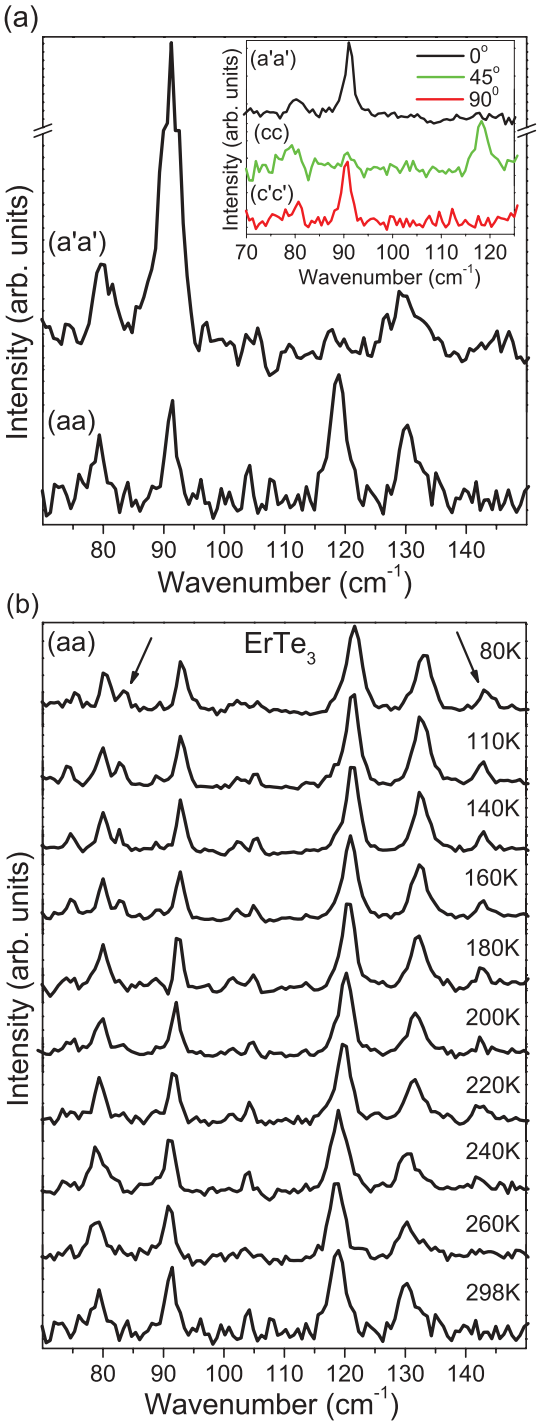

FIG. 3. (Color online) (a) Raman scattering spectra of $ErTe_3$ single crystals measured at room temperature in parallel polarization for different sample orientations, where $a = [100]$, $c = [001]$, $a' = \frac{1}{\sqrt{2}}[101]$, and $c' = \frac{1}{\sqrt{2}}[10\bar{1}]$. Inset shows Raman scattering spectra of $ErTe_3$ measured for three different sample orientations. (b) Raman scattering spectra of $ErTe_3$ measured at different temperatures. New modes in the CDW state are denoted with arrows.

Raman active modes ($3A_{1g} + B_{1g}$) to be observed in the (010) plane. A correlation diagram between crystal (orthorhombic) and layer (tetragonal) symmetries is presented in Fig. 2. According to the Raman tensors for tetragonal symmetry (Fig. 2), the B_{1g} symmetry mode has an intensity-change periodicity of 90°. From the selection rules, we have found that the B_{1g}symmetry mode is Raman active (in the parallel polarization configuration) for all orientations of the sample, except $a'a'$ and $c'c'$. This is in agreement with our experimental findings. In this way, we can assign the P_4 mode of $ErTe_3$ (peak around 120 cm^{-1}) as the B_{1g} symmetry mode of the $ErTe_3$ slab. This means that the 90° periodicity change of P_4 mode intensity is not related with CDW state, as proposed in Ref. 13. Rather it is a consequence of the dominant role of $ErTe_3$ layers in the optical properties of the crystal. The peaks at 132, 92, and 80 cm^{-1} can be assigned as the A_{1g} symmetry modes of the $ErTe_3$ slab.

We cannot exclude the twining effect as a cause of tetragonal symmetry dominance in Raman spectra of $ErTe_3$. Namely, because of the weak interlayer van de Waals bonding, b-axis stacking faults can appear, resulting in twin formation. Such single crystals often can have regions for which the a and c axes are exchanged, and a sample exhibits an average fourfold symmetry, even though it really comprises a superposition of two orthogonal orthorhombic symmetries.

$ErTe_3$ exhibits two successive second-order phase transitions upon cooling at $T_{CDW_1} = 265$ K and $T_{CDW_2} = 158$ K,[12] followed by the modulation of electronic charges and unidirectional and bidirectional ground-state formation.[7] According to Landau's theory of second-order phase transitions, for each second-order phase transition, a characteristic order parameter can be introduced. In the case of CDW formation, the order parameter is the CDW gap. Temperature dependance of the CDW gap can be written as $\Delta(T)/\Delta(0) \sim (1 - T/T_{CDW})^{\beta}$, where β is the critical exponent.

Temperature dependancies of the energy of the 92 cm^{-1} (A_{1g}) and 120 cm^{-1} (B_{1g}) modes of $ErTe_3$ are shown in Fig. 4. The temperature-induced anharmonicity effect[19,20] cannot describe changes of slope at T_{CDW_1} and T_{CDW_2}. Thus we must assume that the changes in energies come from charge redistributions in the second-order phase transition. According to theoretical predictions for the Raman modes, active in the normal phase, the energy change induced by second-order phase transition is proportional to the square of order parameter

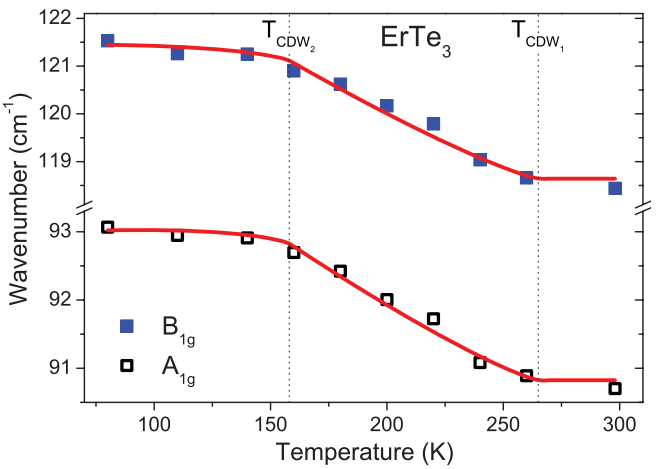

FIG. 4. (Color online) Energy of the Raman active phonons of $ErTe_3$ for the undistorted structure as a function of temperature. Solid lines represent calculated spectra using Eq. (2).

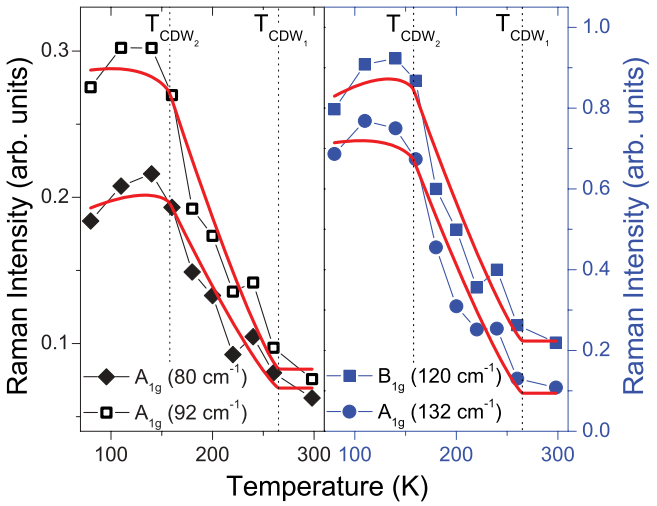

FIG. 5. (Color online) Integrated intensity of the Raman active phonons of $ErTe_3$ for the undistorted structure as a function of temperature. Solid lines represent calculated spectra using Eq. (4).

(CDW gap)[21] $\Delta\omega(T) \sim \Delta(T)^2$. Having this in mind, for the energy shift induced by the second-order phase transition, for $T < T_{CDW_i}$, we obtain

$$\Delta\omega(T)_{CDW_i} = A_i(1 - T/T_{CDW_i})^{2\beta}, \quad (1)$$

where A_i is a coupling constant. If we neglect the interaction between two CDWs,[10] we can approximate the total change of the mode energy, Raman active in the "mother" phase (normal state), with

$$\omega(T) = \omega_0 + \Delta\omega_{CDW_1} + \Delta\omega_{CDW_2}, \quad (2)$$

where ω_0 is a constant. Solid lines in Fig. 4 represent the calculated spectra using Eq. (2). An excellent agreement with the experimental data has been achieved for $\beta = 0.30(2)$, which is also in a complete agreement with the results ($\beta = 0.3$) obtained in Refs. 11 and 14. This is not surprising since amplitudon mode is nothing but the transverse fluctuation of the order parameter. This provides clear evidence for the tight coupling between the CDW gap and the Raman active modes.

Figure 5 shows the temperature dependance of the intensity of the four modes, Raman active for the undistorted structure. One can see that all four modes exhibit the same type of temperature dependence of the intensity. According to Ref. 21, change of intensity of the Raman mode upon the second-order phase transition for the nondegenerate modes, Raman active in the mother phase, is proportional to the square of order parameter $\Delta I(T) \sim \Delta(T)^2$. For $T < T_{CDW_i}$, we obtain

$$\Delta I(T)_{CDW_i} = B_i(1 - T/T_{CDW_i})^{2\beta}, \quad (3)$$

where B_i is a coupling constant. By neglecting interaction between CDWs,[10] we can approximate the Raman intensity temperature change of the modes, Raman active in the mother phase, with

$$I(T) = I_0 + \Delta I_{CDW_1} + \Delta I_{CDW_2}, \quad (4)$$

where I_0 is a constant. The spectra calculated using Eq. (4) for $\beta = 0.3$ [solid lines in Fig. 5] scale rather well with the experimental data. This gives us additional evidence of coupling between Raman modes and the CDW gaps.

Formation of the CDW state is followed by the development of a modulation in the density of the electronic charges which do not transform according to the symmetry group that describes the ionic positions. Owing to the Brillouin-zone folding and lowering the symmetry, new modes became observable in the distorted state. Because of the nature of the second-order phase transition, one does not expect a sudden appearance or disappearance of phonons. In the vicinity of the phase transition, these modes additionally lose intensity and broaden because of fluctuations of the order parameter. In the CDW state of the $ErTe_3$, we have observed additional modes [denoted with arrows in Fig. 3(b)] at 143 cm^{-1} and 83 cm^{-1} that cannot be assigned within the undistorted structure. We concluded that these modes are the consequence of the distortions. Although theory predicts a large number of such modes, many of them cannot be observed because of mode overlapping and their weak intensity.

IV. CONCLUSION

The vibrational properties of $ErTe_3$ were investigated using Raman spectroscopy and were analyzed on the basis of the RTe_3 crystal structure. We have concluded that vibrations of the RTe_3 layers play a dominant role in the optical properties of the crystal. Four Raman active phonons predicted by FGA of the layer symmetry were observed and assigned. Temperature dependence of the energies and intensities of the modes, Raman active for the undistorted structure, have clearly shown coupling of phonons to the CDWs. Theoretical calculations perfectly map experimental data for the critical exponent $\beta = 0.3$. In the distorted state of $ErTe_3$, additional Raman modes have been observed.

ACKNOWLEDGMENTS

This work was supported by the Serbian Ministry of Science and Technological Development under Project No. 141047, No. ON171032, and No. III45018. Part of this work was carried out at the Brookhaven National Laboratory, which is operated for the Office of Basic Energy Sciences, US Department of Energy, by Brookhaven Science Associates (DE-Ac02-98CH10886).

*Present address: Ames Laboratory and Department of Physics and Astronomy, Iowa State University, Ames, IA 50011.

[1] E. DiMasi, M. C. Aronson, J. F. Mansfield, B. Foran, and S. Lee, Phys. Rev. B **52**, 14516 (1995).
[2] N. Ru and I. R. Fisher, Phys. Rev. B **73**, 033101 (2006).
[3] A. Sacchetti *et al.*, Phys. Rev. B **79**, 201101 (2009).
[4] A. Sacchetti, E. Arcangeletti, A. Perucchi, L. Baldassarre, P. Postorino, S. Lupi, N. Ru, I. R. Fisher, and L. Degiorgi, Phys. Rev. Lett. **98**, 026401 (2007).
[5] C. Malliakas, S. J. L. Billinge, H. J. Kim, and M. G. Kanatzidis, J. Am. Chem. Soc. **127**, 6510 (2005).

[6]C. Malliakas and M. G. Kanatzidis, J. Am. Chem. Soc. **128**, 12612 (2006).
[7]N. Ru, C. L. Condron, G. Y. Margulis, K. Y. Shin, J. Laverock, S. B. Dugdale, M. F. Toney, and I. R. Fisher, Phys. Rev. B **77**, 035114 (2008).
[8]H. Yao, J. A. Robertson, E.-A. Kim, and S. A. Kivelson, Phys. Rev. B **74**, 245126 (2006).
[9]V. Brouet, W. L. Yang, X. J. Zhou, Z. Hussain, N. Ru, K. Y. Shin, I. R. Fisher, and Z. X. Shen, Phys. Rev. Lett. **93**, 126405 (2004).
[10]R. G. Moore, V. Brouet, R. He, D. H. Lu, N. Ru, J.-H. Chu, I. R. Fisher, and Z. X. Shen, Phys. Rev. B **81**, 073102 (2010).
[11]R. V. Yusupov, T. Mertelj, J.-H. Chu, I. R. Fisher, and D. Mihailovic, Phys. Rev. Lett. **101**, 246402 (2008).
[12]F. Pfuner, P. Lerch, J.-H. Chu, H.-H. Kuo, I. R. Fisher, and L. Degiorgi, Phys. Rev. B **81**, 195110 (2010).
[13]M. Lavagnini *et al.*, Phys. Rev. B **78**, 201101 (2008).
[14]M. Lavagnini, H.-M. Eiter, L. Tassini, B. Muschler, R. Hackl, R. Monnier, J.-H. Chu, I. R. Fisher, and L. Degiorgi, Phys. Rev. B **81**, 081101 (2010).
[15]E. DiMasi, B. Foran, M. C. Aronson, and S. Lee, Chem. Mater. **6**, 1867 (1994).
[16]B. K. Norling and H. Steinfink, Inorg. Chem. **5**, 1488 (1966); D. J. Haase, H. Steinfink, and E. J. Weiss, *ibid.***4**, 541 (1965).
[17]E. A. Wood, Bell System Tech. J. **43**, 541 (1964); Bell Telephone System Tech. Publ. Monogr. No. 4680, 1964 (unpublished); A. Burneau, J. Raman Spectrosc. **25**, 289 (1994).
[18]Z. V. Popović, Phys. Rev. B **32**, 2382 (1985); R. Zallen, M. L. Slade, and A. T. Ward, *ibid.* **3**, 4257 (1971).
[19]N. Lazarević, Z. V. Popović, R. Hu, and C. Petrovic, Phys. Rev. B **81**, 144302 (2010).
[20]M. Balkanski, R. F. Wallis, and E. Haro, Phys. Rev. B **28**, 1928 (1983).
[21]J. Petzelt and V. Dvořák, J. Phys. C **9**, 1571 (1976).